Using Small Samples to Evaluate Normative Reference Ranges for Retinal Imaging Measures

William H. Swanson, PhD, FAAO,[1]* Brett J. King, OD, FAAO,[1] and Douglas G. Horner, OD, PhD, FAAO[1]

SIGNIFICANCE: Retinal nerve fiber layer (RNFL) deviation maps often incorrectly score healthy eyes as having wedge defects. This study shows how to identify such problems early in the development of normative databases.

PURPOSE: After reference values are embedded in devices, clinicians and researchers often learn about issues that cause false-positive rates in healthy eyes. Here we show a way to detect and address such issues early on.

METHODS: The thickness of the RNFL was measured for both eyes of 60 healthy younger adults aged 20 to 31 years and one eye each of 30 healthy older adults aged 54 to 82 years. Deviation maps were developed from the left eyes of the first 30 younger adults, and between-subject variability in the shape of the RNFL was assessed. This was repeated in their right eyes, in the second group of younger adults and in the older adults.

RESULTS: For the first group of 30 healthy young adults, between-subject variability in the location of the region of greatest thickness meant that 58% of the pixels below the fifth percentile in the left eyes were from four people whose deviation maps had wedge-shaped patterns, as did the deviation maps for the nine right eyes with 87% of the pixels below the fifth percentile. Wedge patterns were also seen in deviation maps for 8 left eyes and 11 right eyes of the second group of young adults and for 9 eyes of the older adults.

CONCLUSIONS: Evaluation of RNFL thickness maps from 30 young adults was sufficient to determine that between-subject variability in the shape of the RNFL can cause wedge patterns in RNFL deviation maps in many healthy eyes.

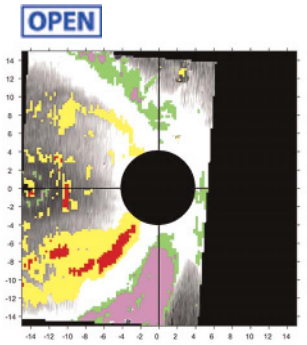

Optom Vis Sci 2019;96:146–155. doi:10.1097/OPX.0000000000001353

Author Affiliations:
[1]Indiana University School of Optometry, Bloomington, Indiana
*wilswans@indiana.edu

As technology advances, new clinical devices often present statistical analyses of data for individual patients based on normative reference values. The goal of these analyses is to have good specificity (low false-positive rates) and good sensitivity (high true-positive rates), but the databases used to produce the normative reference values are often proprietary. This means that false-positive rates can only be determined over time as clinicians and researchers discover factors that can produce high false-positive rates. Statistical properties of probability maps for perimetry have been investigated for three decades,[1–6] but the statistical properties of probability maps for retinal imaging are not as well understood. It is clear that imaging confronts us with a new set of problems: many more locations with probability values, greater correlation between neighboring locations, different variability properties, and different sources of apparent spatial patterns of damage in what are actually healthy eyes.[7] This study shows an example of how such problems can be detected early by testing a relatively small number of healthy eyes in young adults. We have previously performed this type of analysis of maps for thickness of the macula,[8] and here we provide a more detailed rationale for our approach as well as assess reproducibility in evaluating statistical properties of maps for thickness of the retinal nerve fiber layer.

Assessment of retinal nerve fiber layer thickness has become a part of diagnosis and care for patients with glaucoma. However, retinal nerve fiber layer thickness is highly variable across people because of variability in embryological and developmental factors. Embryological processes produce far more retinal ganglion cells than the visual cortex can support, and approximately half of retinal ganglion cells do not establish appropriate connections with visual cortex and die of apoptosis.[9] These embryological processes result in an approximately twofold range in number of retinal ganglion cells in young adults[10] and an approximately twofold range of retinal nerve fiber layer thicknesses.[11] Growth of the eye from infancy to adulthood also results in different sizes of the eye, which is another source of variability in clinical measurement of retinal nerve fiber layer thickness.[12] A further source of variability in retinal nerve fiber layer thickness measurements is variation in vascular anatomy.[13] These factors result in substantial between-subject variability in retinal nerve fiber layer thicknesses of adults in good ocular health, which limits the ability of retinal nerve fiber layer thickness to detect early glaucomatous damage and contributes to discordance between imaging and perimetric results in patients with glaucoma.[14]

Optical coherence tomography is widely used to measure circumpapillary retinal nerve fiber layer thickness using a single scan in a circle around the optic disc. Results for an individual patient are compared with fifth and first percentiles derived from a normative database, and this analysis often yields artifacts.[15,16] In time, it became possible to make many line scans across a rectangular area containing the disc and provide a two-dimensional

retinal nerve fiber layer thickness map. For several devices, retinal nerve fiber layer thickness "deviation maps" have been developed, which flag pixels as yellow or red based on reference values for the fifth and first percentiles of normative databases, respectively. These maps have made it possible to look for spatial patterns of retinal nerve fiber layer damage across the retina.[17] However, just as with circumpapillary retinal nerve fiber layer thickness, there is substantial between-subject variability in retinal nerve fiber layer structure for healthy eyes.[18]

The goal of deviation maps is to help doctors identify glaucomatous retinal nerve fiber layer defects.[19] Identification of glaucomatous damage with deviation maps was first used for static automated perimetry as a way to help clinicians assess patterns of visual field damage. For perimetry, for each visual field location tested, the measured log sensitivity is used to compute difference from mean normal ("deviation"). For each deviation, a probability value is assigned based on how often deviations as large as this are found in the normative database for that location. Test-retest variability in perimetry is as large as between-subject variability,[1] so in healthy eyes any pattern of flagged locations on a perimetric deviation map will change from one test to the next. This means that a small group of contiguous locations with sensitivities less than the 5% or 1% reference values will only be considered a defect if repeated tests flag similar locations.

When deviation maps were introduced for en face retinal nerve fiber layer thickness, they were constructed in an analogous manner as perimetry. However, unlike perimetric deviation maps, repeatable false-positive results are relatively common for retinal nerve fiber layer thickness deviation maps. One study found that 28% of people free of eye disease were identified as having retinal nerve fiber layer wedge defects.[17] Test-retest variability of retinal nerve fiber layer thickness measures is much lower than between-subject variability,[20] so if patients have a wedge-shaped pattern on a retinal nerve fiber layer thickness deviation map on one visit, they are very likely to have it on all future visits.

We demonstrate that this problem could have been identified by testing 30 healthy young adults before testing the hundreds of people needed to develop normative reference ranges for clinical devices. Our approach for evaluating normal between-subject variability is to first assess variability in the outcome of embryological and developmental processes by evaluating between-subject variability in a group of young adults.[8] We looked to see whether most of the locations with thickness below the fifth percentile for a group were from a subset of that group and whether those locations appeared in patterns consistent with glaucomatous damage.

METHODS

Participants

We tested both eyes of 60 healthy young adults in the age range 20 to 31 years with a mean (standard deviation) of 24 (2) years. We tested one eye each of 30 healthy older adults in the age range 54 to 82 years with a mean (standard deviation) of 67 (9) years. Details of inclusion and exclusion criteria have been published elsewhere.[21] Briefly, subjects were required to have had a recent comprehensive eye examination with findings such as normal retinal characteristics, clear ocular media, corrected monocular distance visual acuity of at least 20/20 (20/40 for those older than 70 years), refractive corrections between spherical equivalents of +2 and –6 diopters, and cylindrical correction within ±3.0 diopters. Subjects with ocular or systemic disease currently affecting visual function were excluded from this study. Eyes with epiretinal membranes were also excluded from this study because the membranes can make retinal thickness measurements unreliable. The research for this study adhered to the tenets of the Declaration of Helsinki and was approved by the institutional review board at Indiana University. Informed consent was obtained from each participant after explanation of the procedures and goals of the study before testing began.

Equipment

An IOLMaster (v5; Carl Zeiss Meditec, Dublin, CA) was used to measure axial length and corneal curvature. A Spectralis (Heidelberg Engineering, Heidelberg, Germany, https://www.heidelbergengineering.com) was used to image the retina and autosegment retinal nerve fiber layer.

Imaging Protocols

For each eye imaged on the Spectralis, spacing along a B-scan was set to 14 μm, spacing between B-scans was set to 30 μm, and each B-scan was averaged across nine frames. Scans were gathered for several fixation locations, and then retinal nerve fiber layer thickness maps for these scans were montaged using a custom program. Details have been published elsewhere.[22–24]

Sample Size

This study used a sample size of 30 subjects in each group to assess between-subject variability in retinal nerve fiber layer structure. As shown in Fig. 1, confidence limits for standard deviation are highly asymmetric for low sample sizes, so variance will usually be underestimated. For a sample size of 30, the 95% confidence interval for a standard deviation of 1.0 is fairly symmetric, 0.8 to 1.3. To decrease the width of this interval by ¼, the sample size would have to be increased to 58; to decrease it by ½, the sample size would have to be increased to 126. A sample size of 30 should be sufficient to detect problems that occur in more than 10% of healthy eyes because the 95% confidence level for 0 of 30 ranges from 0 to 11%.

Data Analysis

The first step for each group of 30 eyes was to follow the approach used in clinical devices and generate 5% and 1% reference values for retinal nerve fiber layer thickness maps. This was done after rotating each retinal nerve fiber layer thickness map so that the disc-fovea line was horizontal. The machine-derived retinal nerve fiber layer thicknesses are produced by image processing techniques that operate on individual B-scans to identify the locations of the top and bottom of the retinal nerve fiber layer by changes in reflectance. We developed software to detect errors in this process by comparing adjoining B-scans and correcting these errors when possible.

To create the retinal nerve fiber layer thickness deviation maps, we rotated each montage so that the line connecting the fovea and the center of the optic disc was horizontal and then placed a grid of 128×128 cells centered on the optic disc, where each cell was a 0.23° by 0.23° square (6×6 pixels). We then excluded the cells within 4° of the center of the optic disc. For each cell in the grid, the retinal nerve fiber layer thickness for a given eye was computed as the average across all 36 pixels included in the cell. If any of the 36 pixels had a segmentation error that could not be corrected automatically or was missing data, the cell was considered invalid and

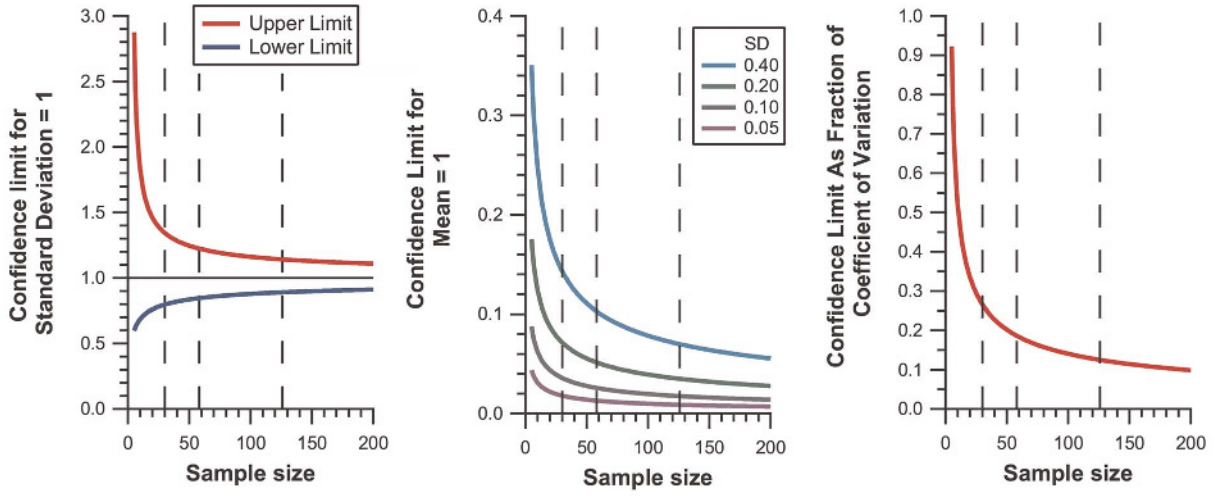

FIGURE 1. Ninety-five percent confidence limits as a function of sample size for SD = 1 (left), mean = 1 (middle), and coefficient of variation (right). Confidence limits are asymmetric for SD, so upper and lower limits are shown separately. Confidence limit for coefficient of variation is shown as fraction of the measured value. Vertical dashed lines show sample sizes of 30, 58, and 126.

was not used. For a given group of 30 eyes, we rejected all cells in the grid that were considered invalid for any 1 of the 30 eyes.

For each cell, we computed the mean and standard deviation across all 30 eyes and used these to compute 5% and 1% reference values for the cell as mean minus 1.640 and 2.326 standard deviations, respectively. When retinal nerve fiber layer thickness for a cell fell below the 5% reference value, it was colored yellow, unless it fell below the 1% reference value, in which case it was colored red. A clinician with expertise in glaucoma (BJK) reviewed these deviation maps and noted when the yellow and red pixels formed a spatial pattern consistent with glaucomatous damage to the retinal nerve fiber layer. This allowed us to assess whether the cells with thicknesses below the 5% reference values were distributed widely across the 30 eyes or were concentrated in a subset of eyes and in spatial patterns consistent with glaucoma.

Group A: 30 Young Adults

We first analyzed data from the left eyes of the first group of 30 young adults and generated reference values for the fifth and first percentiles for each cell from the mean and standard deviation for that cell. Then we applied these reference values to each of the 30 eyes they were derived from, to assess whether ~5% of cells had retinal nerve fiber layer thicknesses below the fifth percentile and whether in some eyes they formed spatial patterns consistent with glaucoma.

To assess reproducibility of the findings in this group, the same methods were applied to their right eyes. We developed reference values based on data from the right eyes and then applied them to create deviation maps for each of these 30 eyes.

Group B: 30 Young Adults

To assess reproducibility of the basic findings, the same approach was used with the second group of 30 young adults. First, the analysis was performed on data from the left eyes, generating reference values from these eyes and then applying them to each of these 30 eyes. Then the analysis was performed on the right eyes, generating reference values from these eyes and then applying them to each of these 30 eyes.

Group C: 30 Older Adults

Finally, to determine whether findings in young adults also applied to older adults, we applied the methods to the data from the older adults. For these people, 22 had the right eye as the study eye, and the data were converted to left eye format by multiplying the *x* axis by −1. Reference values for the fifth and first percentiles were generated from these 30 eyes and then applied to each of these 30 eyes.

Secondary Analyses

As a secondary analysis of factors affecting between-subject variability, effects of axial length on retinal nerve fiber layer thickness were assessed separately for each of the five groups of 30 eyes. For each cell that was valid for all 30 eyes of a group, we correlated retinal nerve fiber layer thickness with axial length of the eye.

In another secondary analysis, between-eye comparisons in retinal nerve fiber layer thickness were conducted in the two groups of young adults. For each eye in a group, we computed a single value for global retinal nerve fiber layer thickness across all cells that were valid for all 30 eyes in that group. In order for readers to be able to compare our findings with those of other kinds of studies of between-eye similarities, we performed linear least squares regression for the global thickness of the left eyes versus global thicknesses of the right eyes and provided R^2 as a measure of effect size. To assess agreement in retinal nerve fiber layer thickness between eyes, we performed Bland-Altman analysis[25] comparing global retinal nerve fiber layer thicknesses of the left and right eyes.

Finally, in compliance with the National Institutes of Health guidelines for investigating sex as a biological variable (https://orwh.od.nih.gov/sex-gender/nih-policy-sex-biological-variable), we generated summary statistics for global retinal nerve fiber layer thickness and axial length separately for women and men.

Data Sharing

In compliance with the National Institutes of Health and Indiana University policies and to protect the confidentiality of our human subject data and protected health information, the Indiana University School of Optometry shares research data in the form of a limited data set pursuant to an approved data use agreement. Data and computer code used in this project will be shared with any research team whose institution executes an approved data use agreement with Indiana University. Interested researchers should contact the Indiana University School of Optometry Office of Compliance and Privacy at 812-855-3402 or optpriv@indiana.edu (http://www.optometry.iu.edu/).

RESULTS

Group A

Fig. 2 shows summary values for retinal nerve fiber layer thickness for the left eyes of the first group of 30 young adults. The left panel shows mean thickness for each cell, with superior and inferior arc-shaped regions of greatest thickness. The middle panel shows standard deviation for each cell, and the right panel shows the coefficient of variation (the standard deviation divided by the mean) for each cell. Standard deviation and coefficient of variation were highest in the regions just outside the arc-shaped regions of greatest thickness, indicating substantial between-subject variability in how far the arcades are from the fovea. For these 30 eyes, 3% of cells fell below the 5% reference value, of which 58% were from four people whose retinal nerve fiber layer thickness deviation maps had clusters of such cells in wedge-shaped patterns (the remaining cells were scattered across 25 people with no consistent pattern).

Fig. 3 shows three examples of individuals with wedge patterns on their retinal nerve fiber layer deviation maps, with conventional use of yellow and red to indicate thicknesses below the fifth and first percentiles, respectively. To better characterize the individual variability, Fig. 3 also uses green and violet to indicate thicknesses greater than the 95th and 99th percentiles, respectively. In the top panel, for the upper arcade of the left eye, there is a cluster of cells thinner than the 5th percentile inside the arcade forming a wedge shape and some cells thicker than the 95th percentile outside the arcade, indicating that the arcade is farther from the fovea than for the mean thickness for the group. The middle panel shows a similar example of wedge-shaped clusters in the upper arcade and a more extreme example in the lower arcade. The bottom panel shows a case where the opposite pattern was found in the lower arcade: there are clusters of cells thicker than the 95th percentile inside the arcade and cells thinner than the 5th percentile outside the arcade, indicating that the arcade was closer to the fovea than for the mean thickness for the group.

Clusters of cells in wedge-shaped patterns were found for the right eyes of this first group of young adults: 4% of cells fell below the 5% reference value, of which 87% were from nine people with wedge patterns due to the location of the arcades. Four of these people also had wedge patterns in the left eye (Fig. 3 includes three examples). The remaining cells were scattered across 20 people with no consistent pattern.

Group B

Clusters of cells in wedge-shaped patterns were found for the second group of young adults: wedge patterns were seen for 8 left eyes and 11 right eyes, which accounted for 66% (left) and 84% (right) of cells below the 5% reference value; the remaining cells were scattered across the remaining eyes with no consistent pattern. Eight people in this group had wedge patterns for both eyes.

Group C

Clusters of cells in wedge-shaped patterns were found for the group of older adults, with 9 eyes having wedge patterns accounting for 72% of cells below the 5% reference value and the rest scattered across 21 eyes with no consistent pattern.

Between-subject variability was slightly higher in the older group than in the young group, as shown in Fig. 4, with the color code indicating the logarithm of the ratio of standard deviations for the group of older adults and for the left eyes of the first young group. The difference in standard deviations for older adults and

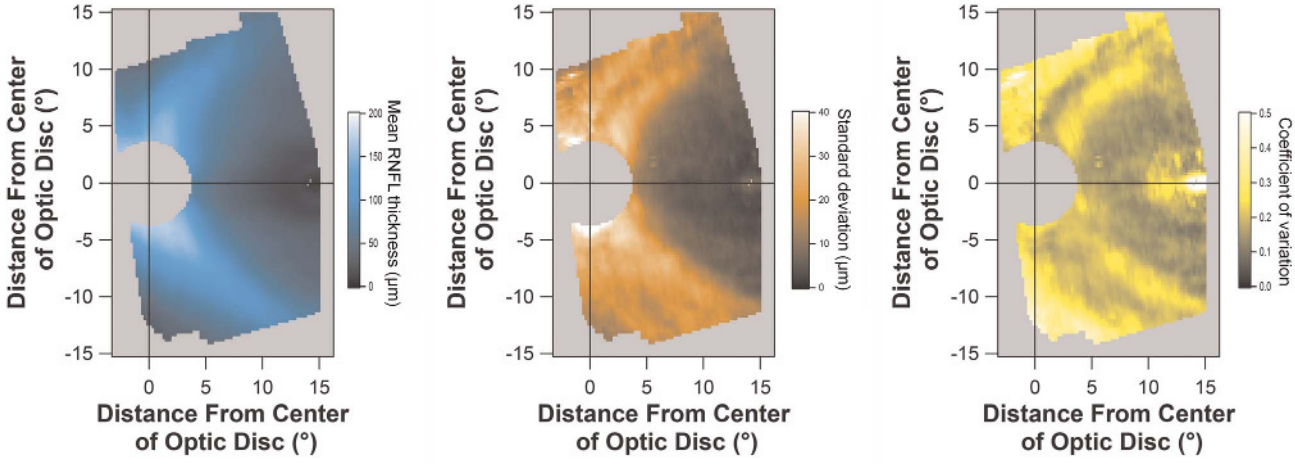

FIGURE 2. Summary values for retinal nerve fiber layer thickness: mean (left), SD (middle), and coefficient of variation (COV; right). These data are for the left eyes of group A, the first group of young adults. Lighter colors indicate greater thickness (left panel) or greater variability (middle and right panels).

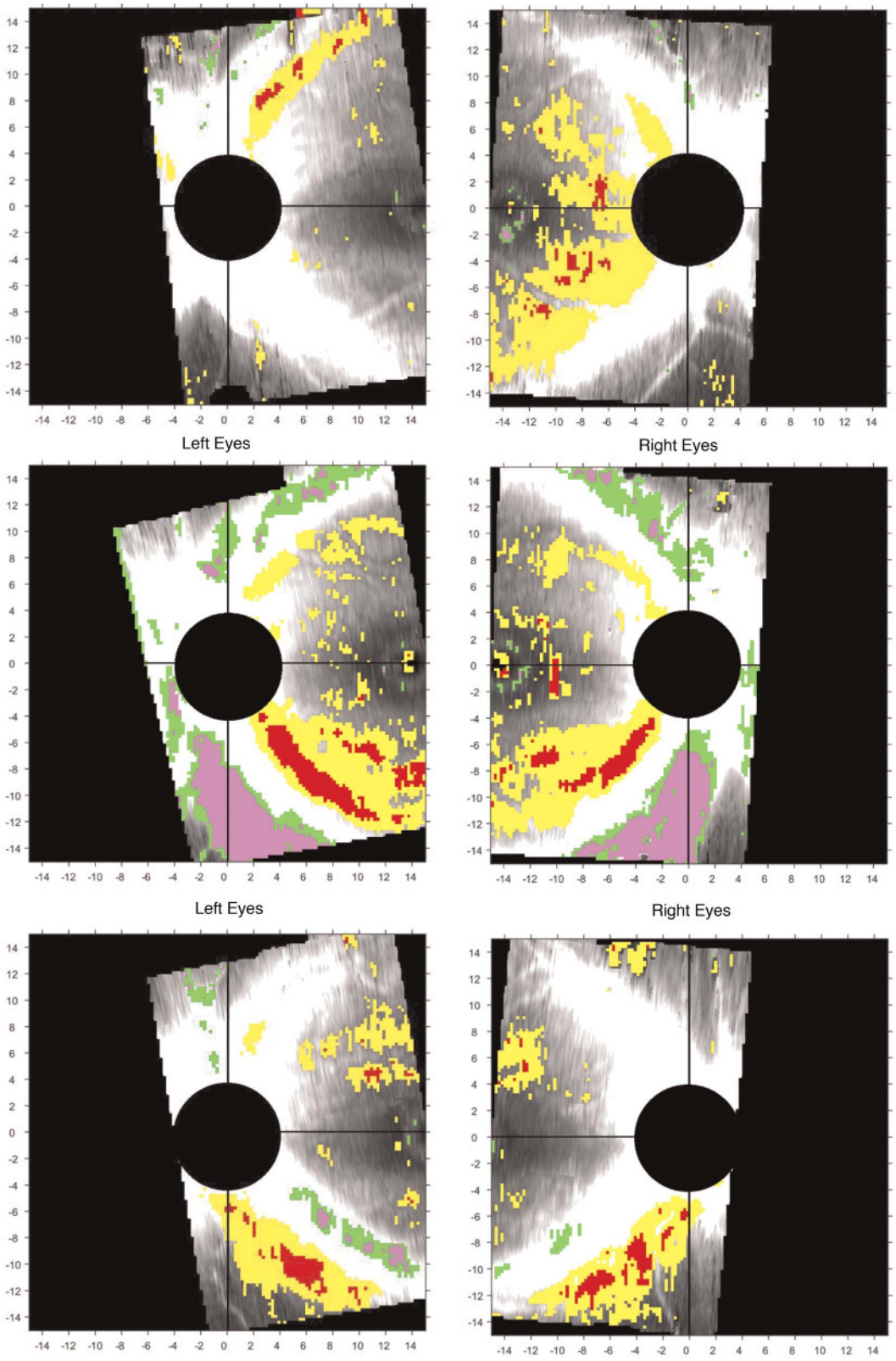

FIGURE 3. Retinal nerve fiber layer deviation maps for the three people in the first group of young controls for whom both eyes had deviation maps showing wedge patterns. Cells below the reference values are shown as red for <1% reference value and yellow for <5% reference value. Cells above the reference values are shown as violet for >99% reference value and green for >95% reference value. Left eyes are shown in the left column and right eyes in the right column.

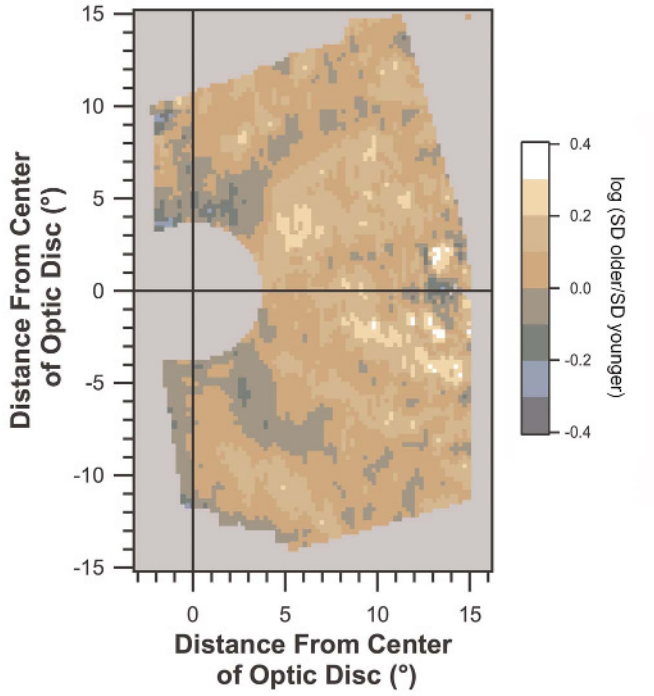

FIGURE 4. Comparison of between-subject variability in young and old eyes. The color code shows the log ratio of SD for retinal nerve fiber layer thickness for the older group (in left eye format) to SD for the left eyes of the first young group. Color scale is shown in the inset.

the left eyes of the first young group had a median of 0.05 log unit, and the interquartile range was 0.00 to 0.11 log unit.

Secondary Analyses

Across the 150 eyes, axial lengths ranged from 22.1 to 27.8 µm. Table 1 shows summary statistics for correlations between retinal nerve fiber layer thickness and axial length for all five sets of eyes. Fig. 5 shows maps of values for Pearson *r* from correlation of retinal nerve fiber layer thickness with axial length for one set of 30 eyes from each of the three groups of people. As axial length increased, retinal nerve fiber layer thickness declined in the outer portions of the arcades but increased many other places, so that median values were near zero.

For the analysis of between-eye differences for young adults in groups A and B, linear least squares regression between global retinal nerve fiber layer thicknesses of the left and right eyes yielded R^2 = 93% for the first group and R^2 = 91% for the second group. Bland-Altman analysis yielded a mean difference of 2 µm for the first group and 1 µm for the second group, with limits of agreement of ±4 µm for both groups.

For the analysis of sex as a biological variable, global thicknesses and axial lengths from the two groups of young adults were combined; there were 38 women and 22 men. For the older adults, there were 15 women and 15 men. Effects of sex as a biological variable for global retinal nerve fiber layer thickness and axial length are shown in Table 2. Effects of sex were not reproducible: median retinal nerve fiber layer thickness was slightly greater for women in the left eyes of young adults but not in the right eyes, and median axial length was slightly smaller for women in the left eyes of young adults but not in the right eyes.

DISCUSSION

In this study, we demonstrated how a relatively small sample size of 30 healthy young adults can be used to assess potential problems in use of normative reference values provided by clinical devices. Machine databases need to include hundreds of adults over a wide range of ages to derive precise estimates of percentiles (Fig. 1). We demonstrated that by testing just 30 young adults it was possible to determine that normal between-subject differences in the locations of the arcades inevitably result in retinal nerve fiber layer thickness deviation maps showing wedge-shaped patterns in a substantial portion of healthy eyes. This approach of testing 30 young adults can be used with other types of imaging data,[8] such as when a large clinic acquires a new imaging device. An understanding of normal between-subject variability can help clinicians and student interns estimate false-positive rates for reference values used in a new device.

We tried to solve this problem with individualized deviation maps by using information on the location of the arcades and the global thickness but failed to find a useful approach. We compared our attempts with a published method using machine learning for superpixel analysis[26] and found that, despite their normalization to the peak retinal nerve fiber layer thickness, diagnostic efficiency was limited: the area under the receiver operating curve was 0.86, which is equivalent to flipping a coin 28% of the time.[27] We infer that, with this structural measurement, deviation maps will not be clinically useful. The clinician will have to perform an expert analysis of the thickness map itself to determine whether the color-coding map shows an artifact, so it is not clear that a deviation map will add anything to expert examination of the raw thickness profile.

Next we looked for potential global indices of retinal nerve fiber layer integrity. For perimetry, a variety of global indices have been developed (e.g., pattern standard deviation, glaucoma hemifield test, and rate of fixation losses) to help clinicians determine whether a pattern seen on a perimetric deviation map is simply due to normal between-subject variability. Similarly, for imaging, it may be helpful to have indices to help clinicians identify when wedge patterns in retinal nerve fiber layer thickness deviation maps are due to normal between-subject variability. To develop such indices, effects of embryological and developmental variability must be addressed. Our approach was to reduce effects of these factors by averaging thicknesses across larger regions. For this step, we analyzed the 5727 cells that were valid for all 60 eyes of the first 30 younger controls,

TABLE 1. Pearson *r* from correlation of RNFL thickness of axial length

	Group A		Group B		
	Left eyes	Right eyes	Left eyes	Right eyes	Group C
Minimum	–0.67	–0.66	–0.58	–0.62	–0.60
Quartile 1	–0.25	–0.23	–0.21	–0.25	–0.15
Median	–0.02	0.04	0.03	0.04	0.11
Quartile 3	0.16	0.18	0.19	0.27	0.24
Maximum	0.67	0.65	0.69	0.72	0.60

Summary statistics are shown for all valid cells of each group. RNFL = retinal nerve fiber layer.

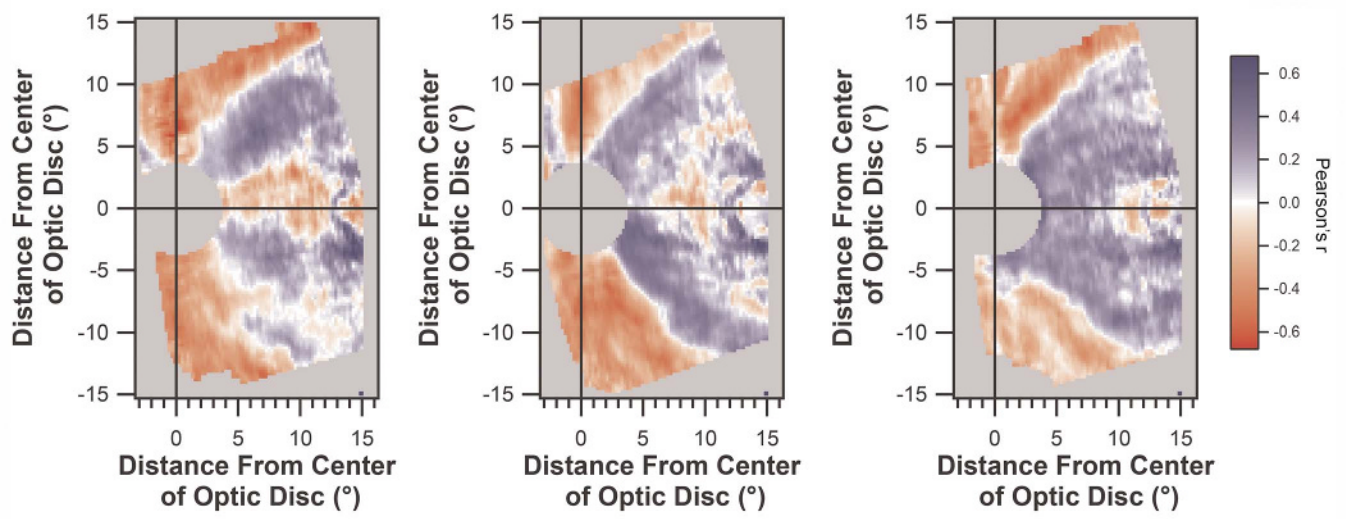

FIGURE 5. Pearson *r* values for correlation of retinal nerve fiber layer thickness with axial length for individual cells. Left panel is for the left eyes for the first group of young adults, middle panel is for the left eyes for the second group of young adults, and right panel is for the older group with data expressed in left eye format for those with the right eye as the study eye.

dividing the cells into five adjoining regions corresponding to projections to five sectors of the optic disc, shown in Fig. 6: superior-nasal, superior-temporal, temporal, inferior-temporal, and inferior-nasal. The mean for thicknesses of all cells in a region was used as the retinal nerve fiber layer thickness for the corresponding disc sector. We evaluated thicknesses for the superior-temporal, temporal, and inferior-temporal sectors and for the global thickness averaged across all five sectors. We also computed thicknesses of superior and inferior halves by averaging across all cells above and below the line connecting the center of the disc with the center of the fovea. Using the mean and standard deviation for each index for each group of 30 eyes, we computed how much retinal nerve fiber layer would need to be lost for someone who began at the mean normal thickness to fall below the fifth percentile. Across the five sets of eyes, the best performance was for global thickness and superior hemifield thickness (where 15 to 18% loss would be required) and for the inferior hemifield thickness (where 16 to 20% loss would be required). For inferior-temporal, superior-temporal, and temporal, loss of 17 to 23% would be required.

It has been suggested that comparison of retinal nerve fiber layer thicknesses of the two eyes of a patient may be another useful index.[28] Therefore, for the 60 young adults, we used Bland-Altman analysis to find the 95% limits of agreement between retinal nerve

TABLE 2. Sex as a biological variable

	Young adults				Older adults	
	Left eyes		Right eyes			
	Female	Male	Female	Male	Female	Male
Global retinal nerve fiber layer thickness (μm)						
Minimum	60	59	57	55	66	56
Quartile 1	70	70	69	69	70	68
Median	74	73	71	72	71	71
Quartile 3	78	77	76	75	76	75
Maximum	91	93	90	93	82	84
Axial length (mm)						
Minimum	22.1	22.3	22.2	22.2	22.2	22.6
Quartile 1	23.3	23.4	23.4	23.4	23.3	23.7
Median	24.1	24.2	24.2	24.2	23.6	24.3
Quartile 3	24.5	24.8	24.9	24.7	25.1	24.9
Maximum	27.0	26.6	27.2	26.5	27.8	26.5

Summary statistics for global retinal nerve fiber layer thickness and axial length for female and male adult groups.

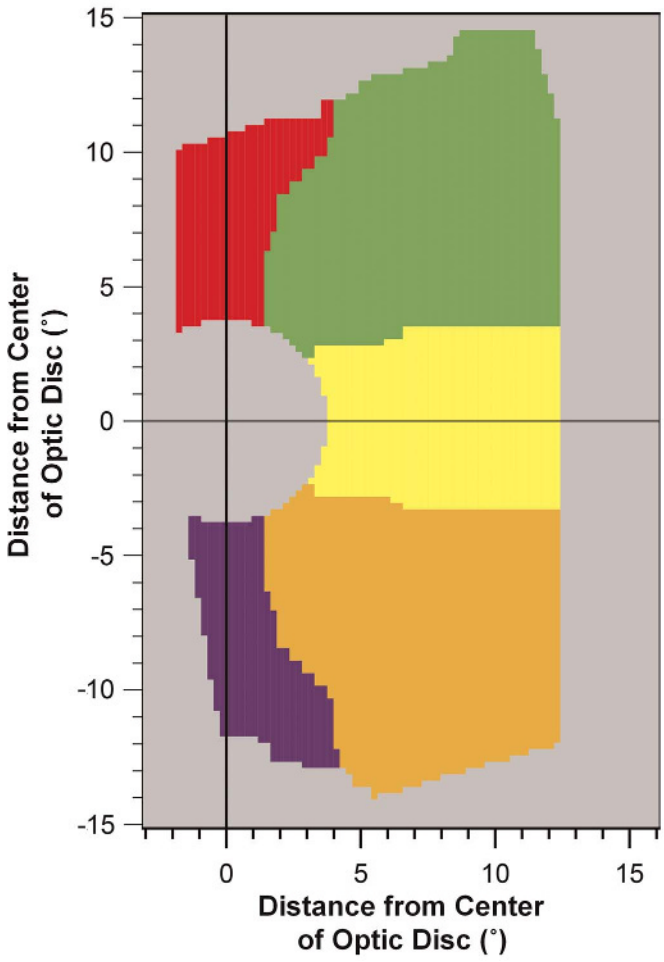

FIGURE 6. Map of retinal nerve fiber layer regions corresponding to five sectors of the optic disc: superior nasal (red), superior temporal (green), temporal (yellow), inferior temporal (orange), and inferior nasal (purple).

fiber layer thicknesses of the two eyes, which ranged from ±4 (global) to ±8 μm (superior-temporal), corresponding to losses of 5 and 10%. We inferred that between-eye comparisons decreased between-subject variability. As shown in Fig. 7, for all six indices, mean thickness was slightly lower for the right eye, and there was a negative slope on the Bland-Altman plot, corresponding to a greater difference in people with thicker retinal nerve fiber layer. We estimated effect size by calculating *z* as the slope estimate divided by the standard deviation of the slope estimate, and effect sizes were modest (–0.6 to –2.9), with the largest effects for the temporal sector (–2.9) and the inferior temporal sector (–2.18).

It is well established that circumpapillary retinal nerve fiber layer thickness is correlated with axial length.[29] To assess whether axial length is likely to provide a useful index of wedge artifacts, we looked at the 14 healthy eyes with severe wedge patterns based on published categories.[17] We found that seven had the region of greatest retinal nerve fiber layer thickness farther from the fovea than for the mean of the group, and seven had it closer to the fovea. For the eyes with greatest retinal nerve fiber layer thickness farther from the fovea, axial lengths ranged from 23.3 to 27.2 mm, with a median of 24.7 mm. For the eyes with greatest retinal nerve fiber layer thickness closer to the fovea, axial lengths ranged from 22.9 to 24.8 mm, with a median of 24.3 mm. By comparison, for the total 120 eyes from younger adults, axial lengths ranged from 22.1 to 27.2 mm, with a median of 24.2 mm.

In portions of the arcades, we found a decline in retinal nerve fiber layer thickness with an increase in axial length but elsewhere found the opposite, with the net effect of axial length on global thickness being minor. Reproducibility of this finding is illustrated in Fig. 5 and Table 1; reproducibility was good for the medians, ranges, and interquartile intervals and in the basic pattern that correlation is negative in the outer portions of the arcades and primarily positive inside the arcades. We inferred that it seems unlikely that axial length would be a useful index.

Although the indices discussed previously have potential to identify glaucomatous damage, they lack the spatial detail about glaucomatous damage that deviation maps attempt to provide. Lack of spatial detail limits the ability to compare retinal nerve fiber layer findings with perimetric findings. An alternate method for obtaining spatial detail in assessing locations of retinal nerve fiber layer damage is evaluation of retinal nerve fiber layer reflectance.[30] Our laboratory has found that reflectance defects can correspond well with perimetric defects.[22,23,31] This means that what seems to be a wedge defect on a reflectance map can be confirmed with targeted perimetry. However, our sample sizes were not large, and we did not have a way to compensate for fixation instability in perimetry, so further work is needed before this becomes a viable option.

We used a sample size of 30 eyes because, for smaller sample sizes, standard deviation can be substantially underestimated because of asymmetric confidence intervals (Fig. 1). We used the example of normative reference values for retinal nerve fiber layer thickness deviation maps, for which it has been previously reported that a substantial percentage of healthy eyes have wedge-shaped patterns on retinal nerve fiber layer thickness deviation maps.[17] We replicated this finding in each of five sets of 30 eyes, finding wedge-shaped patterns in 4, 9, 8, 11, and 9 eyes, respectively. What is new here is not the finding that wedge patterns frequently occur in retinal nerve fiber layer thickness deviation maps for healthy eyes, but rather that this problem could be found by studying only 30 people. The finding was then replicated on another 120 eyes in groups of 30, so it seems likely that other laboratories could find it by studying only 30 people.

The history of the initial finding of wedge patterns in retinal nerve fiber layer thickness deviation maps for healthy eyes is that hundreds of people free of eye disease were tested to establish reference values for deviation maps; these reference values were embedded in devices, and later when researchers compared patients and controls free of eye disease, the problem was uncovered. Had this type of study of 30 young adults been conducted at the outset, the problem could have been identified early on, and approaches could have been developed that could help clinicians decide when a wedge pattern on an retinal nerve fiber layer thickness deviation map may be attributed to normal between-subject variability in the location of the arcades.

In summary, by imaging 30 young adults in good ocular health, we showed that normal between-subject variability of retinal nerve fiber layer structure produces wedge patterns in retinal nerve fiber layer thickness deviation maps for healthy eyes. We analyzed data from groups of 30 healthy eyes to assess reproducibility and so that the findings could be readily replicated by others.

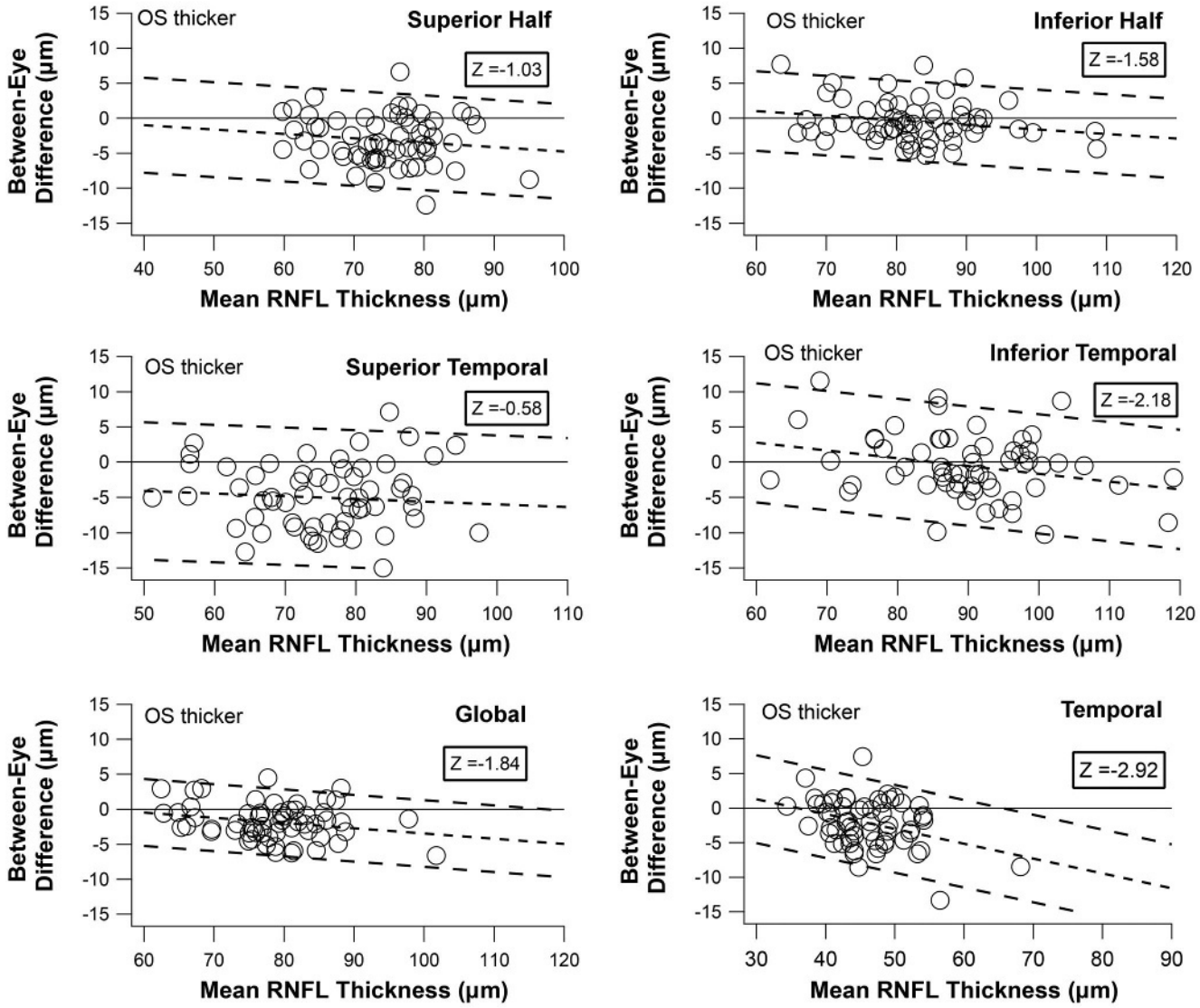

FIGURE 7. Bland-Altman plots for between-eye agreement of six thicknesses: three sectors (superior temporal, temporal, inferior temporal), a global average including all five sectors shown in Fig. 6, and averages for superior and inferior halves. Dashed lines show mean and 95% limits of agreement for linear regression of difference versus mean, and *z* scores are shown for the slope.

ARTICLE INFORMATION

Submitted: April 16, 2018

Accepted: October 31, 2018

Funding/Support: National Eye Institute (R01EY028135; to WHS) and National Eye Institute (R01EY024542; to WHS). The content is solely the responsibility of the authors and does not necessarily represent the official views of the National Institutes of Health.

Conflict of Interest Disclosure: A financial conflict of interest exists in that Heidelberg Engineering provided proprietary software for exporting raw data from the Spectralis, but provided no financial or material support and had no role in the study design, conduct, analysis and interpretation, or writing of the report. WHS is an unpaid consultant for Carl Zeiss Meditec and Heidelberg Engineering. He affirms that these relationships had no impact on this research or on the production of the article. BJK and DGH have no potential conflicts of interest to disclose.

Author Contributions: Conceptualization: WHS, BJK; Formal Analysis: WHS, BJK; Funding Acquisition: WHS; Investigation: WHS; Methodology: WHS, BJK, DGH; Resources: WHS; Supervision: WHS; Visualization: DGH; Writing – Original Draft: WHS; Writing – Review & Editing: BJK, DGH.

REFERENCES

1. Heijl A, Lindgren G, Olsson J. Normal Variability of Static Perimetric Threshold Values across the Central Visual Field. Arch Ophthalmol 1987;105:1544–9.

2. Heijl A, Asman P. A Clinical Study of Perimetric Probability Maps. Arch Ophthalmol 1989;107:199–203.

3. Funkhouser AT, Fankhauser F, Weale RA. Problems Related to Diffuse versus Localized Loss in the Perimetry of Glaucomatous Visual Fields. Graefes Arch Clin Exp Ophthalmol 1992;230:243–7.

4. Wild JM, Pacey IE, Hancock SA, et al. Between-algorithm, Between-individual Differences in Normal Perimetric

Sensitivity: Full Threshold, FASTPAC, and SITA. Swedish Interactive Threshold Algorithm. Invest Ophthalmol Vis Sci 1999;40:1152–61.

5. Artes PH, Hutchison DM, Nicolela MT, et al. Threshold and Variability Properties of Matrix Frequency-doubling Technology and Standard Automated Perimetry in Glaucoma. Invest Ophthalmol Vis Sci 2005;46:2451–7.

6. Turpin A, McKendrick AM. What Reduction in Standard Automated Perimetry Variability Would Improve the Detection of Visual Field Progression? Invest Ophthalmol Vis Sci 2011;52:3237–45.

7. Asrani S, Essaid L, Alder BD, et al. Artifacts in Spectral-domain Optical Coherence Tomography Measurements in Glaucoma. JAMA Ophthalmol 2014;132:396–402.

8. Alluwimi MS, Swanson WH, Malinovsky VE. Between-subject Variability in Asymmetry Analysis of Macular Thickness. Optom Vis Sci 2014;91:484–90.

9. Provis JM, van Driel D, Billson FA, et al. Human Fetal Optic Nerve: Overproduction and Elimination of Retinal Axons during Development. J Comp Neurol 1985;238: 92–100.

10. Curcio CA, Allen KA. Topography of Ganglion Cells in Human Retina. J Comp Neurol 1990;300:5–25.

11. Maurice C, Friedman Y, Cohen MJ, et al. Histologic RNFL Thickness in Glaucomatous versus Normal Human Eyes. J Glaucoma 2016;25:447–51.

12. Savini G, Barboni P, Parisi V, et al. The Influence of Axial Length on Retinal Nerve Fibre Layer Thickness and Optic-disc Size Measurements by Spectral-domain OCT. Br J Ophthalmol 2012;96:57–61.

13. Hood DC, Fortune B, Arthur SN, et al. Blood Vessel Contributions to Retinal Nerve Fiber Layer Thickness Profiles Measured with Optical Coherence Tomography. J Glaucoma 2008;17:519–28.

14. Ashimatey BS, Swanson WH. Between-subject Variability in Healthy Eyes as a Primary Source of Structural-functional Discordance in Patients with Glaucoma. Invest Ophthalmol Vis Sci 2016;57:502–7.

15. Chong GT, Lee RK. Glaucoma versus Red Disease: Imaging and Glaucoma Diagnosis. Curr Opin Ophthalmol 2012;23:79–88.

16. Liu Y, Simavli H, Que CJ, et al. Patient Characteristics Associated with Artifacts in Spectralis Optical Coherence Tomography Imaging of the Retinal Nerve Fiber Layer in Glaucoma. Am J Ophthalmol 2015;159:565–76.e2.

17. Leung CK, Lam S, Weinreb RN, et al. Retinal Nerve Fiber Layer Imaging with Spectral-domain Optical Coherence Tomography: Analysis of the Retinal Nerve Fiber Layer Map for Glaucoma Detection. Ophthalmology 2010;117:1684–91.

18. Leung CK, Yu M, Weinreb RN, et al. Retinal Nerve Fiber Layer Imaging with Spectral-domain Optical Coherence Tomography: Interpreting the RNFL Maps in Healthy Myopic Eyes. Invest Ophthalmol Vis Sci 2012; 53:7194–200.

19. Suh MH, Yoo BW, Kim JY, et al. Quantitative Assessment of Retinal Nerve Fiber Layer Defect Depth Using Spectral-domain Optical Coherence Tomography. Ophthalmology 2014;121:1333–40.

20. Ghasia FF, El-Dairi M, Freedman SF, et al. Reproducibility of Spectral-domain Optical Coherence Tomography Measurements in Adult and Pediatric Glaucoma. J Glaucoma 2015;24:55–63.

21. Swanson WH, Malinovsky VE, Dul MW, et al. Contrast Sensitivity Perimetry and Clinical Measures of Glaucomatous Damage. Optom Vis Sci 2014;91:1302–11.

22. Alluwimi MS, Swanson WH, Malinovsky VE, et al. A Basis for Customising Perimetric Locations within the Macula in Glaucoma. Ophthalmic Physiol Opt 2018;38:164–73.

23. Alluwimi MS, Swanson WH, Malinovsky VE, et al. Customizing Perimetric Locations Based on En Face Images of Retinal Nerve Fiber Bundles with Glaucomatous Damage. Tran Vis Sci Tech 2018;7:5.

24. Ashimatey BS, King BJ, Swanson WH. Retinal Putative Glial Alterations: Implication for Glaucoma Care. Ophthalmic Physiol Opt 2018;38:56–65.

25. Bland JM, Altman DG. Statistical Methods for Assessing Agreement between Two Methods of Clinical Measurement. Lancet 1986;1:307–10.

26. Xu J, Ishikawa H, Wollstein G, et al. Three-dimensional Spectral-domain Optical Coherence Tomography Data Analysis for Glaucoma Detection. PLoS One 2013;8:e55476.

27. Massof RW, Emmel TC. Criterion-free Parameter-free Distribution-independent Index of Diagnostic Test Performance. Appl Optics 1987;26:1395–408.

28. Mwanza JC, Durbin MK, Budenz DL, et al. Interocular Symmetry in Peripapillary Retinal Nerve Fiber Layer Thickness Measured with the Cirrus HD-OCT in Healthy Eyes. Am J Ophthalmol 2011;151: 514–21.e1.

29. Patel NB, Wheat JL, Rodriguez A, et al. Agreement between Retinal Nerve Fiber Layer Measures from Spectralis and Cirrus Spectral Domain OCT. Optom Vis Sci 2012;89:E652–66.

30. Gardiner SK, Demirel S, Reynaud J, et al. Changes in Retinal Nerve Fiber Layer Reflectance Intensity as a Predictor of Functional Progression in Glaucoma. Invest Ophthalmol Vis Sci 2016;57:1221–7.

31. Ashimatey BS, King BJ, Malinovsky VE, et al. Novel Technique for Quantifying Retinal Nerve Fiber Bundle Abnormality in the Temporal Raphe. Optom Vis Sci 2018;95:309–17.